Research Square

Preprints are preliminary reports that have not undergone peer review.
They should not be considered conclusive, used to inform clinical practice,
or referenced by the media as validated information.

GCH1 acts in Parkinson's disease through function rather than abundance

Yu Wang
PLA Navy General Hospital
Yuxian Zhong
Chinese PLA General Hospital
Yu Ding
PLA Navy General Hospital
yu wang
wayu77@126.com

Chinese PLA General Hospital

Research Article

Keywords: GCH1, BH4, tetrahydrobiopterin, tyrosine hydroxylase, dopamine, MPP+, dopaminergic degeneration, Parkinson's disease

Posted Date: November 24th, 2026

DOI: https://doi.org/10.21203/rs.3.rs-11628712/v1

License: This work is licensed under a Creative Commons Attribution 4.0 International License.
Read Full License

Additional Declarations: No competing interests reported.

GCH1 acts in Parkinson's disease through function rather than abundance

Yu Wang[1†], Yuxian Zhong[1†], Yu Ding[1], Yu Wang[2*]

[1] Department of Traditional Chinese Medicine, The Sixth Medical Center, Chinese PLA General Hospital, Beijing, China

[2] The Eighth Medical Center, Chinese PLA General Hospital, Beijing, China

[*]Correspondence: Yu Wang, The Eighth Medical Center, Chinese PLA General Hospital, Beijing, China. E-mail: wayu77@126.com

[†]These authors contributed equally to this work.

Keywords: *GCH1*; BH4; tetrahydrobiopterin; tyrosine hydroxylase; dopamine; MPP+; dopaminergic degeneration; Parkinson's disease

Running title: *GCH1* function in PD

Abstract

GTP cyclohydrolase 1 (*GCH1*) is the rate-limiting enzyme of tetrahydrobiopterin (BH4) synthesis, the essential cofactor of tyrosine hydroxylase (TH) for dopamine production. How this enzyme contributes to Parkinson's disease (PD), through altered abundance or altered function and regulation, remains unresolved. We re-interpret the *GCH1*–BH4 axis by integrating protein atlases, single-nucleus RNA-seq of the human substantia nigra, regulatory and protein–protein interaction networks, a seven-cohort meta-analysis, quantitative proteomics, and MPP+ transcriptomics. *GCH1* is enriched in dopaminergic neurons and functionally central, but not topologically dominant, in the BH4→dopamine axis. Although *GCH1* mRNA is downregulated in PD substantia nigra, protein abundance is unchanged and MPP+ induces compensatory upregulation. Concordantly, an expression quantitative trait locus (QTL) is uncorrelated with PD risk, whereas a splicing QTL generating a catalytically inactive isoform colocalizes with PD risk. These findings reframe

the *GCH1*–BH4 axis from abundance-driven to regulation-centric, with implications for BH4-targeted strategies in PD.

Introduction

The progressive degeneration of nigral dopaminergic neurons is a core pathological feature of Parkinson's disease (PD) [1, 2]. Dopamine synthesis depends on tyrosine hydroxylase (TH), whose catalytic activity requires its cofactor tetrahydrobiopterin (BH4) [3]; BH4 deficiency therefore impairs dopamine synthesis and is considered important for dopaminergic neuronal function.

The rate-limiting enzyme of de novo BH4 synthesis is GTP cyclohydrolase 1 (*GCH1*) [4]. The clearest human evidence for the functional importance of the *GCH1*–BH4 axis comes from dopa-responsive dystonia (DRD), in which loss-of-function *GCH1* mutations deplete BH4, impair TH activity, and reduce dopamine synthesis [5, 6, 7, 8]. In the PD substantia nigra, transcriptomic studies have reported downregulation of dopaminergic genes [10] and single-nucleus RNA-seq has confirmed depletion of TH-expressing dopaminergic neurons [11], although bulk-tissue downregulation may partly reflect neuronal loss rather than cell-autonomous regulation. Yet the prevailing interpretation, that reduced *GCH1* abundance drives dopaminergic vulnerability, rests on precisely this bulk-tissue downregulation.

In addition to genetic association studies [12], recent functional work has established that the *GCH1*–BH4 pathway is neuroprotective in dopaminergic neurons: Gch1 ablation depletes BH4 and dopamine and causes dopaminergic degeneration, and BH4 augmentation by sepiapterin is protective [13]; Gch1 deficiency additionally impairs TH homeostasis [14]. Whether *GCH1* instead acts in PD through its functional state, splicing isoforms, stress responsiveness, and upstream regulation, rather than through abundance, has not been systematically resolved.

To address this gap, we performed a multi-omics re-interpretation of the *GCH1*–BH4 axis using public resources: protein expression and disease annotations from the Human Protein Atlas (HPA), Genotype-Tissue Expression (GTEx) co-expression, two single-nucleus RNA-seq atlases of the human substantia nigra (GSE140231 and GSE157783), a curated regulatory network, a protein–protein interaction network, bulk co-expression validation, quantitative proteomics, and MPP+ transcriptomics. Our aim was to separate an abundance

effect from a splicing-dependent functional effect, re-interpreting the role of this known enzyme rather than nominating *GCH1* as a novel risk gene.

Results

GCH1 is specifically enriched in dopaminergic neurons, and the BH4/dopamine module is dopaminergic-neuron-intrinsic (Figure 1, Figure 2, and Supplementary Figure S5)

Human Protein Atlas (HPA) [15] RNA expression data show that the dopaminergic markers TH, SLC6A3 and SLC18A2 are highly expressed in the midbrain (which contains the substantia nigra), and HPA disease annotations link *GCH1* to parkinsonism, dystonia and phenylketonuria, consistent with the established role of *GCH1* in BH4 biosynthesis and tyrosine hydroxylase function (Figure 1). Complementing these expression data, single-cell transcriptomics of the mouse midbrain localize Gch1 to a subset of dopaminergic neurons [13], and GTEx co-expression data confirm that *GCH1* and TH are co-expressed in the human substantia nigra [9]. Consistent with this, we analyzed a published single-nucleus RNA-seq atlas of the human substantia nigra (GSE140231) [16]: across 6,105 nuclei from five control donors, *GCH1* was detected in 28.3% of TH-positive dopaminergic neurons and in 38.8% of neurons co-expressing TH and SLC6A3, compared with only 2.6% of TH-negative cells (Figure 2). At higher resolution, the fraction of *GCH1*-positive nuclei increased progressively with dopaminergic identity, from 2.6% in TH-negative cells to 15.4% in TH+/SLC6A3− neurons and 38.8% in TH+/SLC6A3+ (canonical) dopaminergic neurons (chi-square $P = 3.8 \times 10{-}79$); within TH+ neurons, *GCH1* co-expressed with the dopaminergic transcription factor NR4A2/NURR1 (Fisher odds ratio = 3.35, P = 0.002), was largely excluded from GABAergic neurons (8.0% vs 38.8% in dopaminergic neurons; Fisher odds ratio = 5.33, $P = 9.5 \times 10{-}8$), and correlated with TH at the single-nucleus level (Spearman $\rho = 0.26$, P = 0.002) (Supplementary Figure S4). To test whether this specificity extends from *GCH1* to the full BH4/dopamine module and to the disease brain, we computed module scores in a second single-nucleus atlas that includes PD patients (GSE157783; 41,435 nuclei from five PD patients and six controls): the BH4-synthesis and dopamine modules were

both strongly enriched in annotated dopaminergic neurons (DaNs) relative to all other cell types, including CADPS2+ neurons, microglia and astrocytes (BH4 module z-score +0.84 in DaNs versus −0.25 in microglia and astrocytes; dopamine module +11.0 versus ≈0; Mann–Whitney U test, all $P < 0.0001$) (Supplementary Figure S5A, B). These database-level observations situate *GCH1* at the interface of BH4 metabolism and dopaminergic neuron function, motivating a systematic multi-omics characterization of the *GCH1*–BH4 axis.

GCH1 is functionally central but not topologically dominant in the BH4→dopamine axis, enriched in the resistant dopaminergic-neuron subtype (Figure 3, Figure 4, and Supplementary Figure S5C)

To characterize the upstream regulatory network of *GCH1*, we curated transcription factors (TFs) governing *GCH1* expression. The transcription factor NRF2 (NFE2L2) directly binds and activates the *GCH1* promoter (chromatin immunoprecipitation-validated) [19], and ATF4 is an upstream regulator of *GCH1* through the integrated stress response [20]. In addition, multiple microRNAs, including miR-1-3p, miR-206, miR-613 and miR-34a-5p, are predicted by ENCORI/starBase with cross-linking immunoprecipitation (CLIP) experimental evidence to target *GCH1* (Figure 3); among these, miR-1-3p is supported by a microarray-based interaction in miRTarBase [28], and miR-34a-5p and miR-206 have been validated as direct *GCH1* targets by luciferase reporter assays, in lung cancer cells [29] and in canine cardiomyocytes [30], respectively; miR-613 remains a candidate that awaits functional validation.

A *GCH1*-centered protein–protein interaction (PPI) network assembled from STRING [18] connected *GCH1* to the BH4 biosynthetic enzymes PTS, SPR, QDPR and PCBD1, the feedback regulator GCHFR, and the dopaminergic markers TH, DDC, SLC6A3 and SLC18A2 (Figure 4A). Topological analysis of this 11-node network placed TH, rather than *GCH1*, at the topological center: TH had the highest degree [9], betweenness (9.94) and closeness (0.909) centrality (empirical $P = 0.000$ by a degree-preserving permutation test), whereas *GCH1* had a degree of 7, betweenness of 1.48 and closeness of 0.769 (each ranked fourth; empirical $P = 0.90$) (Figure 5C), confirming that *GCH1* is not a topological hub. This is biologically consistent with *GCH1* acting as the upstream rate-

limiting enzyme of BH4 synthesis, functionally central through flux limitation rather than topologically dominant, whereas TH is the downstream convergence point at which BH4 is consumed for dopamine synthesis. As an expression-based reverse validation in two independent bulk substantia nigra cohorts (GSE7621, n = 25; GSE20292, n = 29) [22, 23], *GCH1* expression was significantly positively correlated with the dopaminergic markers DDC, SLC6A3 and SLC18A2, and with PTS, in both cohorts (e.g., SLC18A2: $\rho = 0.69$ and 0.77; PTS: $\rho = 0.56$ and 0.65; all $P < 0.05$), and with TH in both cohorts (GSE7621: $\rho = 0.78$, $P < 0.001$; GSE20292: $\rho = 0.47$, $P = 0.009$), whereas correlations with SPR, QDPR and GCHFR were weak (Figure 4B). When stratifying by disease status, the *GCH1*–TH co-expression coupling was attenuated in PD: in GSE7621 the correlation was positive but stronger in controls ($\rho = 0.97$, $P < 0.001$) than in PD ($\rho = 0.70$, $P = 0.003$), and in GSE20292 it was lost entirely in PD ($\rho = -0.10$) while persisting in controls ($\rho = 0.59$, $P = 0.010$) (Supplementary Figure S2); DDC and SLC6A3 showed a similar PD-associated attenuation in GSE20292. This pattern indicates that *GCH1* co-expresses primarily with the dopaminergic axis in the control substantia nigra, and that this transcriptional coupling is attenuated in PD, consistent with its enrichment in dopaminergic neurons (Figure 2). Consistently, within DaNs of the PD-including atlas (GSE157783), the resistant CALB1+ subtype was selectively enriched for the *GCH1*–BH4 axis: *GCH1* positivity was higher in CALB1+ than in CALB1− DaNs (72% versus 51%; $P = 0.011$), as were TH (100% versus 67%; $P = 8.3 \times 10-5$), the dopaminergic transcription factor NR4A2 (88% versus 47%; $P = 3.3 \times 10-5$), and the BH4 module score (+0.257 versus −0.131; $P = 3.8 \times 10-4$) (Supplementary Figure S5C).

GCH1 acts in PD through function rather than abundance

Consistent with a functional rather than an abundance-driven role, *GCH1* protein abundance in post-mortem PD substantia nigra did not significantly differ from controls in a published quantitative proteomic dataset (15 PD vs. 15 controls) [31]. Extending this to the full BH4/dopamine protein module, all six BH4 biosynthetic enzymes were unchanged in PD substantia nigra (*GCH1*, $q = 0.718$; PTS, $q = 0.745$; SPR, $q = 0.243$; QDPR, $q = 0.258$; PCBD1, $q = 0.740$; GCHFR, $q = 0.453$), whereas the dopaminergic synthesis and transport proteins were significantly reduced (TH, $q = 7.96 \times 10^{-4}$; DDC, $q = 0.029$; SLC6A3, $q < 0.0001$; SLC18A2, $q < 0.0001$) (Figure 5A). This protein-level

pattern mirrors the transcriptomic meta-analysis and indicates that surviving nigral cells retain their BH4-synthetic capacity while dopaminergic proteins decline with neuronal loss, further supporting a functional rather than abundance-driven role for *GCH1*. Likewise, a public transcriptomic dataset of differentiated dopaminergic SH-SY5Y cells exposed to 1-methyl-4-phenylpyridinium (MPP+) (GSE203522) showed compensatory upregulation of *GCH1* (log2 fold change = +0.43, $P < 0.001$), together with upregulation of the integrated stress response transcription factor ATF4 (log2 fold change = +1.07, $P < 0.001$) (Supplementary Figure S1) [32]. This stress-responsive, compensatory induction of *GCH1* is consistent with the reported neuroprotective role of *GCH1*/BH4 upregulation in the 6-OHDA model [33]. Independent reverse validation supported the regulatory and protein-abundance findings but qualified the MPP+ stress response. The NRF2–*GCH1* axis was independently confirmed, as Nrf2 knockdown in microglia reduced *GCH1* expression and BH4 generation [24]. A random-effects meta-analysis (DerSimonian–Laird) of *GCH1* mRNA across seven substantia nigra cohorts (n = 7; 77 PD and 68 controls) confirmed consistent downregulation (pooled log2 fold change = −0.83, 95% CI −1.09 to −0.56, $P < 0.0001$, $I^2 = 7.3\%$; Figure 5D), with all seven cohorts showing the same direction of effect, consistent with the unchanged protein abundance [31]. Leave-one-out sensitivity analysis confirmed that this pooled estimate was robust to the exclusion of any single cohort (range −0.73 to −0.89, all $P < 0.05$), and the funnel plot showed no marked asymmetry (Supplementary Figure S7). In the GSE20163 cohort (one of the seven meta-analyzed cohorts; 8 PD and 9 controls) [23], this pattern was recapitulated in detail: *GCH1* mRNA was significantly lower in PD (log2 fold change = −1.06, $P = 3.8 \times 10^{-4}$; Supplementary Figure S6), together with concordant downregulation of the dopaminergic markers TH (log2 fold change = −1.77, $P = 0.002$), SLC18A2 (−2.89, $P = 0.002$), SLC6A3 (−1.44, $P = 0.007$) and DDC (−0.89, $P = 0.032$), and a modest reduction of PTS (−0.30, $P = 0.015$), whereas the other BH4 biosynthetic enzymes SPR, QDPR, PCBD1 and GCHFR, and the regulators NRF2 and ATF4, were unchanged. Across all seven cohorts, the meta-analysis likewise showed robust downregulation of the dopaminergic axis: TH (pooled log2 fold change = −1.85, $P = 0.0002$, $I^2 = 80.6\%$), SLC18A2 (−2.40, $P < 0.0001$, $I^2 = 64.3\%$), SLC6A3 (−1.76, $P < 0.0001$, $I^2 = 55.7\%$) and DDC (−0.80, $P < 0.0001$, $I^2 = 38.4\%$), together with a modest reduction of PTS (−0.40, $P < 0.0001$, $I^2 =$

0%), whereas the other BH4 biosynthetic enzymes (SPR, QDPR, PCBD1, GCHFR) and the regulators NRF2 and ATF4 were unchanged (Figure 5D). This selective co-downregulation of *GCH1* with the dopaminergic axis, rather than with the entire BH4 pathway, is consistent with dopaminergic-neuron loss rather than a primary *GCH1* deficit, further supporting a functional rather than abundance-driven role. In contrast, in a second, independent MPP+ dataset of undifferentiated SH-SY5Y cells (GSE151808) [25], MPP+ activated the integrated stress response (ATF4 and DDIT3/CHOP upregulation) but did not induce *GCH1* (log2 fold change = −0.10, P = 0.700; Supplementary Figure S3), unlike the differentiated dopaminergic SH-SY5Y model (GSE203522), in which *GCH1* was upregulated [32]. This cell-context dependence indicates that the compensatory *GCH1* stress response requires a dopaminergic/differentiated background, further supporting the dopaminergic-neuron enrichment of *GCH1*. Direct genetic evidence supports this function-over-abundance interpretation: a recent neopterin genome-wide association study (GWAS) resolved the *GCH1* locus into two independent signals, an expression QTL that raises *GCH1* mRNA (rs140884539) and a splicing QTL (rs12323905/rs11158026) that increases a catalytically inactive 213-amino-acid *GCH1* isoform, and only the splicing QTL colocalized with PD risk, whereas the expression QTL did not [34]. We independently verified these QTL annotations in GTEx v8: rs12323905 and rs11158026 are significant *GCH1* splicing QTLs (whole-blood normalized effect size −0.33 and −0.31, $P = 3.6 \times 10^{-9}$ and 3.4×10^{-8}, respectively), and rs140884539 is a *GCH1* expression QTL with a consistently negative effect direction across 20 tissues including brain, corroborating the expression-versus-splicing distinction resolved by the GWAS (Figure 5B). In the substantia nigra specifically, *GCH1* bulk expression is too low for the tissue to be an eGene or sGene, so the splicing direction could not be measured directly in nigral tissue; nonetheless, the GTEx results independently confirm that the two PD-associated variants act through splicing rather than expression, reinforcing a function-over-abundance mechanism. Thus, raising *GCH1* expression alone is not associated with PD, whereas altering *GCH1* function through splicing is, directly supporting a functional rather than abundance-driven role.

A non-cell-autonomous layer: dopaminergic neurons show a wired-but-minimal NRF2 antioxidant program, and candidate glia-to-DaN signals are identified

Because *GCH1* is transcriptionally activated by NRF2 and ATF4 (Figure 3), we next examined the oxidative-stress axis across cell types in the PD-including atlas (GSE157783). Dopaminergic neurons expressed the NRF2 transcription factor NFE2L2 (detected in 84% of DaNs), yet its canonical downstream effectors NQO1 (8%) and HMOX1 (4%) were barely detected; in contrast, microglia showed high HMOX1 expression (23%; $P = 1.1 \times 10{-}11$ versus DaNs) (Figure 6A). This wired-but-minimal NRF2 program in dopaminergic neurons, transcription factor present, antioxidant effectors minimal, suggests that oxidative-stress handling is largely delegated to glia, whereas dopaminergic neurons depend on their intrinsic BH4/dopamine axis. As a sensitivity analysis for potential transcript drop-out, we benchmarked NQO1 and HMOX1 against positive-control DaN markers (mean detection 60.0%; e.g., TH 78.4%, SLC18A2 83.8%) and negative-control genes (mean 16.6%; e.g., ALB 2.7%, CD3D 0%, MOG 4.1%): the detection of NQO1 (8.1%) and HMOX1 (4.1%) was far below the positive-control baseline and close to the negative controls. Low-rank matrix imputation (ALRA) showed that part of this under-detection is technical, imputation raised the detection of NQO1 and HMOX1 (to ~100% and ~96%, respectively), yet their imputed expression remained extremely low (mean log1p 0.12 and 0.09, respectively), still well below NFE2L2 itself in DaNs (log1p 1.14) and below microglial HMOX1 (log1p 0.21). Thus, even allowing for drop-out, the NRF2 antioxidant effectors are expressed at negligible levels in dopaminergic neurons relative to the transcription factor and to microglia, supporting a wired-but-minimal rather than an absolute on/off program. Consistent with non-cell-autonomous regulation, ligand–receptor co-expression identified candidate glia-to-DaN signals: the microglial ligands SPP1 (86.6% of microglia) and TGFB1 (44.7%) with the DaN receptors ITGAV/ITGB1 and TGFBR1/TGFBR2, and the astrocytic ligand FGF2 (56.4%) with FGFR1 (56.8% of DaNs); IGF1R was detected on 91.9% of DaNs (Figure 6D). A permutation test (1,000 random relabelings of cell-type identities) showed that all six ligand–receptor co-expression scores were significantly higher than expected by chance (empirical $P \leq 0.006$). These candidates nominate glial signals that may impinge on the NRF2–ATF4–*GCH1* axis, although their functional

relevance remains to be validated. Within dopaminergic neurons, stratification by disease showed that the BH4 module was higher in PD than control DaNs (z-score +0.15 vs −0.20, P = 0.002), as was the NRF2 module (+0.11 vs −0.15, P = 0.048), whereas the ATF4 module showed a trend (+0.07 vs −0.09, P = 0.067), consistent with compensatory upregulation in surviving PD dopaminergic neurons. Consistent with the enrichment of *GCH1* in the resistant DaN subtype, CALB1-positive DaNs showed higher *GCH1* detection and expression than CALB1-negative DaNs in both PD and control (PD: 76.2% vs 66.7% detection; mean log1p 1.00 vs 0.75; control: 50.0% vs 39.3%), although the CALB1-positive subpopulation was largely restricted to PD donors (21 of 25 cells), limiting cross-disease inference (Figure 6B). At the cell-type level, the PD atlas showed marked glial expansion (microglia 14.2% versus 5.4% in controls and astrocytes 13.5% versus 9.6%), together with a proportional reduction of oligodendrocytes (44.9% vs 56.8%), supporting a non-cell-autonomous, gliosis-associated component in PD (Figure 6C).

Discussion

The central contribution of this work is not the identification of *GCH1*, long established as the BH4 rate-limiting enzyme, but a re-interpretation of how it participates in PD, separating an abundance effect from a splicing-dependent functional effect. Integrating protein expression and disease annotations, single-nucleus transcriptomics, regulatory and interaction networks, and expression validation, four layers emerged: (i) *GCH1* and the BH4/dopamine module are specifically enriched in dopaminergic neurons; (ii) *GCH1* is the rate-limiting enzyme of the BH4 pathway, both upstream (NRF2/ATF4 regulation and miRNA targeting) and within the pathway (PPI network and co-expression with dopaminergic markers), and is further enriched in the resistant CALB1+ subtype; (iii) the role of *GCH1* in PD is functional rather than abundance-driven, as its protein abundance is unchanged in PD substantia nigra while MPP+ induces compensatory upregulation and genetic evidence ties PD risk to a splicing (function-altering) rather than an expression QTL; and (iv) a non-cell-autonomous layer, in which dopaminergic neurons show a wired-but-minimal NRF2 antioxidant program while glia bear the oxidative-stress response, and candidate glia-to-DaN signals are identified (Figure 7).

The single-nucleus RNA-seq data show that *GCH1* is detected in 38.8% of TH+/SLC6A3+ dopaminergic neurons but only 2.6% of TH-negative cells, indicating that *GCH1* expression is closely tied to the dopaminergic identity. This is consistent with GTEx co-expression of *GCH1* and TH in the substantia nigra and with mouse single-cell data localizing Gch1 to dopaminergic neurons [13]. The significant positive co-expression of *GCH1* with TH, DDC, SLC6A3 and SLC18A2 in bulk substantia nigra transcriptomes further supports the tight coupling of *GCH1* to the dopamine synthetic and transport machinery. The progressive increase in *GCH1* positivity across dopaminergic identity (TH+/SLC6A3− < TH+/SLC6A3+), the co-expression with the dopaminergic transcription factor NR4A2/NURR1, and the exclusion from GABAergic neurons (Supplementary Figure S4) further sharpen this dopaminergic-neuron specificity. Extending this specificity from the single gene to the pathway, module scoring in the PD-including atlas (GSE157783) showed that the BH4 and dopamine modules are selectively enriched in DaNs relative to all other cell types, and that within DaNs the resistant CALB1+ subtype carries the highest *GCH1*–BH4 axis, consistent with a neuroprotective role.

The regulatory network positions *GCH1* downstream of NRF2 (NFE2L2), which directly binds the *GCH1* promoter, and of ATF4 through the integrated stress response. These regulators converge on the cellular response to oxidative and metabolic stress, suggesting that *GCH1* expression is actively regulated rather than constitutively fixed. The miRNA–*GCH1* interactions retrieved from ENCORI/starBase are candidate post-transcriptional regulators, several of which now have independent experimental support: miR-1-3p by microarray and miR-34a-5p and miR-206 by luciferase reporter assays (in lung cancer cells and canine cardiomyocytes, respectively). Notably, among the predicted *GCH1*-targeting miRNAs, miR-34a-5p has been implicated in dopaminergic neurotoxicity, and *GCH1* knockdown itself remodels the microRNA profile in microglia, including miR-133a-3p [35], indicating bidirectional *GCH1*–miRNA regulatory relationships. Consistent with a convergent post-transcriptional mechanism, miR-34a is upregulated in the 6-OHDA-induced PD model, where it negatively regulates the NRF2 pathway and reduces dopaminergic cell survival [36]. Because miR-34a-5p is also a validated direct *GCH1* target [29], its upregulation could concurrently attenuate both NRF2 and *GCH1*, two upstream

components of the *GCH1*–BH4 axis characterized here, providing a candidate mechanism that tilts the axis toward functional insufficiency. Notably, miR-34 family members are context-specifically regulated: miR-34b/c are downregulated in the PD brain [37], whereas miR-34a is upregulated in PD models, so these inferences are restricted to miR-34a. Owing to the fact that public substantia nigra miRNA expression datasets with sufficient power are limited, these predicted interactions could not be evaluated at the expression level in this study; whether miR-34a-5p or miR-133a-3p functionally target *GCH1* specifically in dopaminergic neurons is a testable priority for future work.

Notably, *GCH1* protein abundance did not significantly differ between PD and control substantia nigra in a published quantitative proteomic dataset, and neither did the other BH4 biosynthetic enzymes (PTS, SPR, QDPR, PCBD1, GCHFR), whereas the dopaminergic proteins TH, DDC, SLC6A3 and SLC18A2 were significantly reduced. A public MPP+ transcriptomic dataset showed compensatory upregulation of *GCH1* together with ATF4. This apparent contrast with classical biochemical studies reporting reduced *GCH1* activity in the PD substantia nigra [38] is consistent with a functional, rather than abundance-driven, contribution: those early measurements reflect total tissue enzyme activity, which declines as dopaminergic neurons are lost, whereas quantitative proteomics assesses tissue-level protein abundance, so the two readouts are not equivalent. Together with the enrichment and hub features above, this indicates that the pathophysiological contribution of *GCH1* is more likely mediated by its functional state and stress responsiveness than by reduced expression per se. Consistent with this, genetic evidence ties *GCH1* to PD through function-affecting rather than expression-reducing variants: rare DRD-related *GCH1* variants are enriched in PD patients and a common haplotype tagged by rs841 is associated with reduced PD risk and higher *GCH1* expression [39], and the rare *GCH1* p.Ser80Asn variant confers PD risk in East Asian populations [40]. Most recently, as described in Results, a neopterin GWAS showed that only a splicing (function-altering) QTL, not an expression QTL, colocalizes with PD risk [34], directly supporting a function-over-abundance mechanism. Together with dopa-responsive dystonia, in which loss-of-function *GCH1* mutations deplete BH4 and impair TH activity [5, 6, 7, 8], these findings suggest that *GCH1* function and regulation, rather than abundance, are the critical determinants in dopaminergic degeneration. Independent

reverse validation further indicated that the compensatory *GCH1* stress response is cell-context dependent, observed in differentiated dopaminergic SH-SY5Y cells (GSE203522) but not in undifferentiated cells (GSE151808), reinforcing the dopaminergic-neuron-specific role of *GCH1*. Although the QTL verification relied on whole-blood splicing QTLs and cross-tissue expression QTLs, because *GCH1* bulk expression in the substantia nigra is too low for that tissue to be an eGene or sGene; this reflects the current boundary of public data; nigral single-cell QTL mapping is needed to measure the splicing direction of rs12323905/rs11158026 directly in dopaminergic neurons.

The main limitation of this study is that it is descriptive and relies entirely on public datasets without any autonomous functional experiments; the predicted regulatory relationships (particularly the miRNA–*GCH1* interactions) and the glia-to-dopaminergic-neuron ligand–receptor signaling are computational predictions that lack experimental validation and should not be read as established mechanisms, and the stress-responsive role of *GCH1* similarly requires functional validation in cellular and animal models. **The splicing QTL–PD colocalization reported here is an indirect inference: the splicing direction of the PD-associated *GCH1* QTL could not be measured directly in nigral tissue, because *GCH1* bulk expression in the substantia nigra is too low for that tissue to be an eGene or sGene, and our verification therefore relied on GTEx whole-blood splicing QTLs and cross-tissue expression QTLs; direct single-cell QTL experiments in the human brain are still needed to confirm expression of this catalytically inactive splicing isoform in dopaminergic neurons.** Furthermore, the CALB1-positive DaN subpopulation was almost entirely derived from PD donors (21 of 25 cells), so **the higher *GCH1* expression in this resistant subtype can only be described as an observation within PD samples, not as evidence that the CALB1+ subtype is intrinsically high in *GCH1*; a cross-disease comparison with sufficient control cells is required before any conclusion about subtype-specific *GCH1* retention can be drawn.** These limitations, however, are not incidental; they reflect the current constraints on human-brain tissue acquisition and sequencing depth, and it is precisely on this basis that the study offers its value: by turning these observational constraints into a falsifiable model, in which *GCH1* acts in PD through its splicing-dependent functional state and stress responsiveness rather than through abundance, the work provides clear, testable directions for future functional

studies, including nigral single-cell QTL mapping and dopaminergic-neuron-specific perturbation of the candidate catalytically inactive *GCH1* isoform. In summary, *GCH1* is a dopaminergic-neuron-enriched, stress-responsive rate-limiting enzyme of the BH4 pathway whose contribution to PD is functional and regulatory rather than abundance-driven, with a non-cell-autonomous glial layer that warrants further study.

Materials and Methods

Public database and single-nucleus RNA-seq analysis

The public resources and datasets analyzed in this study are summarized in Table 1. *GCH1* protein expression in human brain tissues and its disease annotations were retrieved from the Human Protein Atlas (HPA) [15]. *GCH1* and TH co-expression in the human substantia nigra was examined using the GTEx portal [9]. For single-nucleus transcriptomic validation, we downloaded a published single-nucleus RNA-seq atlas of the human substantia nigra (GEO accession GSE140231) [16], comprising 6,105 nuclei from five control donors. For each nucleus, TH-positive neurons were defined as TH count > 0, and dopaminergic neurons (DaN) as TH count > 0 and SLC6A3 count > 0; *GCH1* positivity was defined as *GCH1* count > 0. To extend these analyses to PD, we additionally analyzed a second single-nucleus RNA-seq atlas of the human midbrain (GSE157783) [17], comprising 41,435 nuclei from five PD patients and six controls with cell-type annotations. In GSE157783, dopaminergic neurons were defined by the author-provided cell-type annotation (DaNs; 74 nuclei), and the detection rate of a gene was defined as the fraction of DaN nuclei with raw count > 0. Module scores for four curated gene sets (BH4 synthesis [*GCH1*, PTS, SPR, QDPR, PCBD1, GCHFR], dopamine synthesis and transport [TH, DDC, SLC6A3, SLC18A2], the NRF2 antioxidant response [NFE2L2, NQO1, HMOX1, GCLC, GCLM], and the ATF4 integrated stress response [ATF4, DDIT3, PPP1R15A, TRIB3, ASNS, CHAC1]) were computed as the mean z-scored log1p-normalized expression of each gene set in each nucleus. Within annotated dopaminergic neurons (DaNs), the resistant (CALB1+) and vulnerable (SOX6+) subtypes were compared for *GCH1* and BH4 module scores. Candidate glia-to-neuron signaling was assessed by co-expression of ligand–receptor pairs (ligand detected in microglia or astrocytes, receptor detected in dopaminergic neurons). The statistical significance of

each ligand–receptor co-expression score (the product of the ligand detection rate in microglia or astrocytes and the receptor detection rate in DaNs) was assessed by permuting cell-type labels 1,000 times while keeping the expression matrix fixed; the empirical P value was the fraction of permutations whose co-expression score was ≥ the observed score. For sensitivity analysis of potential transcript drop-out, the GSE157783 count matrix was imputed with ALRA (adaptively-thresholded low-rank approximation). Specifically, the log1p-transformed count matrix was decomposed by rank-30 truncated singular value decomposition to capture the low-rank expression structure, and a threshold was set at the 1st percentile of the reconstructed values at the observed non-zero entries, below which reconstructed values were set to zero to distinguish true biological expression from drop-out noise; detection rate was recomputed after imputation, and imputed expression was benchmarked against NFE2L2 in DaNs and HMOX1 in microglia.

Regulatory network, protein-protein interaction and expression correlation validation

The *GCH1*-centered protein–protein interaction (PPI) network was assembled with STRING (version 12.0) [18] using a medium-confidence combined score threshold of 0.4. Transcription factors regulating *GCH1* were curated from direct experimental evidence: NRF2/NFE2L2 (chromatin immunoprecipitation-validated binding to the *GCH1* promoter) [19] and ATF4 (an upstream regulator through the integrated stress response) [20]. MicroRNAs targeting *GCH1* were retrieved from ENCORI/starBase [21], filtered for CLIP experimental evidence (clipExpNum ≥ 1) and at least two target-prediction algorithms, and the top evidence-ranked miRNAs were visualized. For expression-based reverse validation, we used bulk substantia nigra expression matrices from two independent cohorts, GSE7621 (16 PD, 9 controls) and GSE20292 (11 PD, 18 controls) [22, 23], and computed Spearman correlation coefficients between *GCH1* and its PPI partners separately in each cohort. To examine whether the *GCH1*–dopaminergic-axis co-expression coupling differs by disease status, we additionally computed these correlations within the PD and control subgroups of each cohort. For independent reverse validation of the three core findings, we additionally (i) curated independent experimental evidence for the NRF2–*GCH1* axis (Nrf2 knockdown reducing *GCH1* and BH4) [24]; (ii) examined

GCH1 mRNA abundance between PD and control substantia nigra in the two bulk cohorts using the Mann–Whitney U test; and (iii) analyzed a second, independent MPP+ transcriptomic dataset of undifferentiated SH-SY5Y cells treated with MPP+ (500 μM or 1 mM, 36 h) in the presence or absence of the SELENOT-mimetic peptide PSELT (GSE151808) [25], comparing *GCH1*, ATF4, DDIT3 and TH across conditions. For external validation, we additionally analyzed a third, independent bulk substantia nigra cohort (GSE20163, 8 PD and 9 controls; HG-U133A microarray) [23] and compared *GCH1*, the BH4 biosynthetic enzymes (PTS, SPR, QDPR, PCBD1, GCHFR), the dopaminergic markers (TH, DDC, SLC6A3, SLC18A2) and the regulators NRF2 and ATF4 between PD and control using Welch's t test and the two-sided Mann–Whitney U test.

Dissecting abundance-versus-function: mRNA–protein decoupling, meta-analysis and splicing-QTL verification

To distinguish whether *GCH1* acts in PD through abundance or through function, we designed three complementary analyses that contrast transcript abundance, protein abundance, and genetic function. First, a cross-cohort random-effects meta-analysis was used to obtain a robust estimate of *GCH1* transcriptional change rather than relying on any single cohort. Per-cohort log2 fold changes (PD vs control) were combined across seven substantia nigra cohorts (GSE7621 [16 PD, 9 controls], GSE20292 [11 PD, 18 controls], GSE20163 [8 PD, 9 controls], GSE20164 [6 PD, 5 controls], GSE8397 [15 PD, 7 controls], GSE20141 [10 PD, 8 controls] and GSE20295 [11 PD, 15 controls]) [22, 23, 26, 27] using a random-effects model (DerSimonian–Laird), which accommodates between-cohort heterogeneity; the between-study variance (τ^2) and the I^2 statistic quantified heterogeneity, and the low I^2 (7.3%) indicated that the downregulation was consistent across cohorts rather than driven by any single study. Sensitivity was assessed by leave-one-out analysis, in which the pooled estimate was recalculated after excluding each cohort in turn. Publication bias was evaluated by visual inspection of the funnel plot (per-cohort log2 fold changes plotted against their standard errors), with asymmetry interpreted as potential small-study effects (Supplementary Figure S7). Second, to test the abundance hypothesis directly, we juxtaposed mRNA and protein readouts in the substantia nigra: the meta-analytic mRNA downregulation was compared against *GCH1*

protein abundance from a published quantitative proteomic dataset (15 PD vs 15 controls) [31], together with the other BH4 biosynthetic enzymes (PTS, SPR, QDPR, PCBD1, GCHFR) and the dopaminergic proteins (TH, DDC, SLC6A3, SLC18A2). The rationale is that if *GCH1* contributes to PD through reduced abundance, mRNA and protein should change concordantly, whereas a dissociation, mRNA downregulated while protein is unchanged, would instead point to a functional or regulatory, rather than abundance-driven, mechanism. Third, to separate an abundance effect from a splicing-dependent functional effect genetically, we interrogated the *GCH1* locus in GTEx (v8): we verified that rs140884539 acts as a *GCH1* expression QTL and that rs12323905 and rs11158026 act as *GCH1* splicing QTLs, consistent with the neopterin GWAS that resolved the locus into an expression QTL uncorrelated with PD risk and a splicing QTL that generates a catalytically inactive 213-amino-acid isoform and colocalizes with PD risk [34].

Statistical analysis

Single-nucleus RNA-seq comparisons of *GCH1* expression between TH-positive and TH-negative cells were performed with the two-sided Mann–Whitney U test, and differences in *GCH1*-positive proportions with the chi-square test or Fisher's exact test (for small subgroups). Spearman rank correlation was used to assess co-expression between *GCH1* and its interaction partners in bulk substantia nigra transcriptomes. Differential expression in the MPP+ transcriptomic dataset was assessed using the published DESeq2 statistics (log2 fold change and adjusted P values), and GSE151808 group comparisons with the two-sided Mann–Whitney U test. A two-sided $P < 0.05$ was considered statistically significant. Analyses were performed with Python 3 (SciPy, pandas, statsmodels).

Data availability

The datasets analyzed in this study are publicly available as follows. The single-nucleus RNA-seq atlases of the human substantia nigra (GSE140231) and midbrain (GSE157783), the bulk substantia nigra transcriptomes (GSE7621, GSE20292, GSE20163, GSE20164, GSE8397, GSE20141 and GSE20295), and the MPP+ transcriptomic datasets (GSE203522 and GSE151808) were obtained from the Gene Expression Omnibus (GEO, ncbi.nlm.nih.gov/geo). Protein expression and disease

annotations were obtained from the Human Protein Atlas (proteinatlas.org) and GTEx (gtexportal.org). The protein–protein interaction network was retrieved from STRING (string-db.org), and the miRNA–*GCH1* interactions from ENCORI/starBase (rnasysu.com).

Code availability

All analyses were performed in Python 3 (SciPy, pandas, statsmodels). The analysis scripts are available from the corresponding author upon reasonable request.

Declarations

Ethical approval

Not applicable. This study used only publicly available datasets and did not involve human participants, animal experiments, or cell lines.

Consent to participate

Not applicable.

Consent to publish

Not applicable.

Author contributions

Yu Wang (first author) and Yuxian Zhong: conceptualization, methodology, investigation, and writing, original draft. Yu Ding: data curation, formal analysis, and validation. Yu Wang (corresponding author): conceptualization, supervision, writing, review and editing. All authors contributed to the article and approved the submitted version.

Funding

The author(s) declare that no financial support was received for the research, authorship, and/or publication of this article.

Competing interests

The authors declare that the research was conducted in the absence of any commercial or financial relationships that could be construed as a potential conflict of interest.

References

1. Kalia, L. V. & Lang, A. E. Parkinson's disease. *Lancet* 386, 896–912 (2015).

2. Poewe, W., Seppi, K., Tanner, C. M., Halliday, G. M., Brundin, P., Volkmann, J. et al. Parkinson disease. *Nat. Rev. Dis. Primers* 3, 17013 (2017).

3. Daubner, S. C., Le, T. & Wang, S. Tyrosine hydroxylase and regulation of dopamine synthesis. *Arch. Biochem. Biophys.* 508, 1–12 (2011).

4. Thöny, B., Auerbach, G. & Blau, N. Tetrahydrobiopterin biosynthesis, regeneration and functions. *Biochem. J.* 347, 1–16 (2000).

5. Ichinose, H., Ohye, T., Takahashi, E., Seki, N., Hori, T., Segawa, M. et al. Hereditary progressive dystonia with marked diurnal fluctuation caused by mutations in the GTP cyclohydrolase I gene. *Nat. Genet.* 8, 236–242 (1994).

6. Blau, N., Bonafé, L. & Thöny, B. Tetrahydrobiopterin deficiencies without hyperphenylalaninemia: diagnosis and genetics of dopa-responsive dystonia and sepiapterin reductase deficiency. *Mol. Genet. Metab.* 74, 172–185 (2001).

7. Furukawa, Y., Kish, S. J., Bebin, E. M., Jacobson, R. D., Fryburg, J. S., Wilson, W. G. et al. Dystonia with motor delay in compound heterozygotes for GTP-cyclohydrolase I gene mutations. *Ann. Neurol.* 44, 10–16 (1998).

8. Segawa, M. Hereditary progressive dystonia with marked diurnal fluctuation. *Brain Dev.* 33, 195–201 (2011).

9. GTEx Consortium. The GTEx Consortium atlas of genetic regulatory effects across human tissues. *Science* 369, 1318–1330 (2020).

10. Grünblatt, E., Mandel, S., Jacob-Hirsch, J., Zeligson, S., Amariglio, N., Rechavi, G. et al. Gene expression profiling of parkinsonian substantia nigra pars compacta;

alterations in ubiquitin-proteasome, heat shock protein, iron and oxidative stress regulated proteins, cell adhesion/cellular matrix and vesicle trafficking genes. *J. Neural Transm.* 111, 1543–1573 (2004).

11. Martirosyan, A., Ansari, R., Pestana, F., Hebestreit, K., Gasparyan, H., Aleksanyan, R. et al. Unravelling cell type-specific responses to Parkinson's disease at single cell resolution. *Mol. Neurodegener.* 19, 7 (2024).

12. Klein, C. & Westenberger, A. Genetics of Parkinson's disease. *Cold Spring Harb. Perspect. Med.* 2, a008888 (2012).

13. Cronin, S. J. F., Yu, W., Hale, A., Licht-Mayer, S., Crabtree, M. J., Korecka, J. A. et al. Crucial neuroprotective roles of the metabolite BH4 in dopaminergic neurons. *Preprint at bioRxiv* https://doi.org/10.1101/2023.05.08.539795 (2023).

14. Larbalestier, H., Keatinge, M., Watson, L., White, E., Gowda, S., Wei, W. et al. GCH1 deficiency activates brain innate immune response and impairs tyrosine hydroxylase homeostasis. *J. Neurosci.* 42, 702–716 (2022).

15. Uhlén, M., Fagerberg, L., Hallström, B. M., Lindskog, C., Oksvold, P., Mardinoglu, A. et al. Proteomics. Tissue-based map of the human proteome. *Science* 347, 1260419 (2015).

16. Agarwal, D., Sandor, C., Volpato, V., Caffrey, T. M., Monzón-Sandoval, J., Bowden, R. et al. A single-cell atlas of the human substantia nigra reveals cell-specific pathways associated with neurological disorders. *Nat. Commun.* 11, 4183 (2020).

17. Smajić, S., Prada-Medina, C. A., Landoulsi, Z., Ghelfi, J., Delcambre, S., Dietrich, C. et al. Single-cell sequencing of human midbrain reveals glial activation and a Parkinson-specific neuronal state. *Brain* 145, 964–978 (2022).

18. Szklarczyk, D., Kirsch, R., Koutrouli, M., Nastou, K., Mehryary, F., Hachilif, R. et al. The STRING database in 2023: protein-protein association networks and functional enrichment analyses for any sequenced genome of interest. *Nucleic Acids Res.* 51, D638–D646 (2023).

19. Xue, J., Yu, C., Sheng, W., Zhu, W., Luo, J., Zhang, Q. et al. The Nrf2/GCH1/BH4 axis ameliorates radiation-induced skin injury by modulating the ROS cascade. *J. Invest. Dermatol.* 137, 2059–2068 (2017).

20. Yang, G., Yang, Y., Song, Z., Chen, L., Liu, F., Li, Y. et al. Spliceosomal GTPase Eftud2 deficiency-triggered ferroptosis leads to Purkinje cell degeneration. *Neuron* 112, 3452–3469 (2024).

21. Li, J. H., Liu, S., Zhou, H., Qu, L. H. & Yang, J. H. starBase v2.0: decoding miRNA-ceRNA, miRNA-ncRNA and protein-RNA interaction networks from large-scale CLIP-Seq data. *Nucleic Acids Res.* 42, D92–D97 (2014).

22. Lesnick, T. G., Papapetropoulos, S., Mash, D. C., Ffrench-Mullen, J., Shehadeh, L., de Andrade, M. et al. A genomic pathway approach to a complex disease: axon guidance and Parkinson disease. *PLoS Genet.* 3, e98 (2007).

23. Zheng, B., Liao, Z., Locascio, J. J., Lesniak, K. A., Roderick, S. S., Watt, M. L. et al. PGC-1α, a potential therapeutic target for early intervention in Parkinson's disease. *Sci. Transl. Med.* 2, 52ra73 (2010).

24. Chen, Y., Li, B., Quan, J., Li, Z., Li, Y. & Tang, Y. Inhibition of ferroptosis by mesenchymal stem cell-derived exosomes in acute spinal cord injury: role of Nrf2/GCH1/BH4 axis. *Neurospine* 21, 642–655 (2024).

25. Alsharif, I., Boukhzar, L., Lefranc, B., Godefroy, D., Aury-Landas, J., Rego, J. D. et al. Cell-penetrating, antioxidant SELENOT mimetic protects dopaminergic neurons and ameliorates motor dysfunction in Parkinson's disease animal models. *Redox Biol.* 40, 101839 (2021).

26. Moran, L. B., Duke, D. C., Deprez, M., Dexter, D. T., Pearce, R. K. & Graeber, M. B. Whole genome expression profiling of the medial and lateral substantia nigra in Parkinson's disease. *Neurogenetics* 7, 1–11 (2006).

27. Zhang, Y., James, M., Middleton, F. A. & Davis, R. L. Transcriptional analysis of multiple brain regions in Parkinson's disease supports the involvement of specific protein

processing, energy metabolism, and signaling pathways, and suggests novel disease mechanisms. *Am. J. Med. Genet. B Neuropsychiatr. Genet.* 137B, 5–16 (2005).

28. Huang, H. Y., Lin, Y. C., Li, J., Huang, K. Y., Shrestha, S., Hong, H. C. et al. miRTarBase 2020: updates to the experimentally validated microRNA-target interaction database. *Nucleic Acids Res.* 48, D148–D154 (2020).

29. Tai, F., Zhai, R., Ding, K., Zhang, Y., Yang, H., Li, H. et al. Long non-coding RNA lung cancer-associated transcript 1 regulates ferroptosis via microRNA-34a-5p-mediated GTP cyclohydrolase 1 downregulation in lung cancer cells. *Int. J. Oncol.* 64, 64 (2024).

30. Wei, J., Zhang, Y., Li, Z., Wang, X., Chen, L., Du, J. et al. GCH1 attenuates cardiac autonomic nervous remodeling in canines with atrial-tachypacing via tetrahydrobiopterin pathway regulated by microRNA-206. *Pacing Clin. Electrophysiol.* 41, 459–471 (2018).

31. Jang, Y., Pletnikova, O., Troncoso, J. C., Pantelyat, A. Y., Dawson, T. M., Rosenthal, L. S. et al. Mass Spectrometry-Based Proteomics Analysis of Human Substantia Nigra From Parkinson's Disease Patients Identifies Multiple Pathways Potentially Involved in the Disease. *Mol. Cell. Proteomics* 22, 100452 (2023).

32. Fiore, N. J., Tamer-Mahoney, J. D., Beheshti, A., Nieland, T. J. F. & Kaplan, D. L. 3D biocomposite culture enhances differentiation of dopamine-like neurons from SH-SY5Y cells: a model for studying Parkinson's disease phenotypes. *Biomaterials* 290, 121858 (2022).

33. Yang, X. X., Wang, G. Q., Wen, Q., Zhao, Y. J., Li, D. D. & Zhang, F. Artemisinin alleviates Parkinson's disease by targeting Adcy5-Gch1 axis to trigger a cascade generation of BH4 and dopamine in rats. *Genome Biol.* 26, 267 (2025).

34. Orrù, V., Marongiu, M., Steri, M., Marongiu, M., Sidore, C., Serra, V. et al. Genetic co-regulation of neopterin and Parkinson's disease. *npj Parkinsons Dis.* 12, 69 (2026). doi: 10.1038/s41531-026-01279-x

35. Jia, S., Chen, G., Liang, Y., Liang, X. & Meng, C. GCH1-regulated miRNAs are potential targets for microglial activation in neuropathic pain. *Biosci. Rep.* 41, BSR20210051 (2021).

36. Ba, Q., Cui, C., Wen, L., Feng, S., Zhou, J. & Yang, K. C. Schisandrin B shows neuroprotective effect in 6-OHDA-induced Parkinson's disease via inhibiting the negative modulation of miR-34a on Nrf2 pathway. *Biomed. Pharmacother.* 75, 165–172 (2015).

37. Miñones-Moyano, E., Porta, S., Escaramís, G., Rabionet, R., Iraola, S., Kagerbauer, B. et al. MicroRNA profiling of Parkinson's disease brains identifies early downregulation of miR-34b/c which modulate mitochondrial function. *Hum. Mol. Genet.* 20, 3067–3078 (2011).

38. Nagatsu, T. & Sawada, M. Biochemistry of postmortem brains in Parkinson's disease: historical overview and future prospects. *J. Neural Transm. Suppl.* 72, 113–120 (2007).

39. Rudakou, U., Ouled Amar Bencheikh, B., Ruskey, J. A., Krohn, L., Laurent, S. B., Spiegelman, D. et al. Common and rare GCH1 variants are associated with Parkinson's disease. *Neurobiol. Aging* 73, 231.e1–231.e6 (2019).

40. Tay, Y. W., Lee, A. L., Schee, J. P., Lin, C. H., Tan, E. K., Shin, J. H. et al. GCH1 p.Ser80Asn confers risk for Parkinson's disease in East Asian populations. *Mov. Disord.* (2026). doi: 10.1002/mds.70530

Tables

Table 1. Summary of public resources and datasets used in this study.

Resource	**Identifier / Accession**	**Description**	**Scale**	**Used in**
Human Protein Atlas (HPA)	proteinatlas.org	Protein expression and disease annotations	Brain regions	Figure 1
GTEx	gtexportal.org	*GCH1*–TH co-expression;	Substantia nigra	Figure 1; Results

		expression QTL/splicing QTL verification		
GSE140231 (Agarwal 2020)	GEO	Single-nucleus RNA-seq, human substantia nigra	6,105 nuclei, 5 controls	Figure 2
GSE157783 (Smajić 2022)	GEO	Single-nucleus RNA-seq, human midbrain	41,435 nuclei, 5 PD, 6 controls	Supplementary Figure S5; Results
STRING v12.0	string-db.org	GCH1 protein–protein interaction network	N/A	Figure 4A
ENCORI/starBase v2.0	rnasysu.com	miRNA–GCH1 interactions (CLIP evidence)	N/A	Figure 3
GSE7621 (Lesnick 2007)	GEO	Bulk substantia nigra mRNA	16 PD, 9 controls	Figure 4B
GSE20292 (Zheng 2010)	GEO	Bulk substantia nigra mRNA	11 PD, 18 controls	Figure 4B
GSE20163 (Zheng 2010)	GEO	Bulk substantia nigra mRNA (external validation)	8 PD, 9 controls	Supplementary Figure S6; Results
PXD037684 (Jang 2023)	ProteomeXchange	Quantitative proteomics, human substantia nigra	15 PD vs 15 controls	Figure 5A; Results
GSE203522 (Fiore 2022)	GEO	MPP+ transcriptome, differentiated SH-SY5Y	2D Ctrl vs 2D MPP+	Supplementary Figure S1

GSE20164 (Zheng 2010)	GEO	Bulk substantia nigra mRNA (meta-analysis)	6 PD, 5 controls	Figure 5D; Results
GSE8397 (Moran 2006)	GEO	Bulk substantia nigra mRNA (meta-analysis)	15 PD, 7 controls	Figure 5D; Results
GSE20141 (Zheng 2010)	GEO	Laser-dissected SNpc neurons (meta-analysis)	10 PD, 8 controls	Figure 5D; Results
GSE20295 (Zhang 2005)	GEO	Bulk substantia nigra mRNA (meta-analysis)	11 PD, 15 controls	Figure 5D; Results
GSE151808 (Alsharif 2021)	GEO	MPP+ transcriptome, undifferentiated SH-SY5Y	500 µM / 1 mM MPP+	Supplementary Figure S3

Abbreviations: CLIP, cross-linking immunoprecipitation; MPP+, 1-methyl-4-phenylpyridinium; SH-SY5Y, human neuroblastoma cell line; N/A, not applicable.

Figure Legends

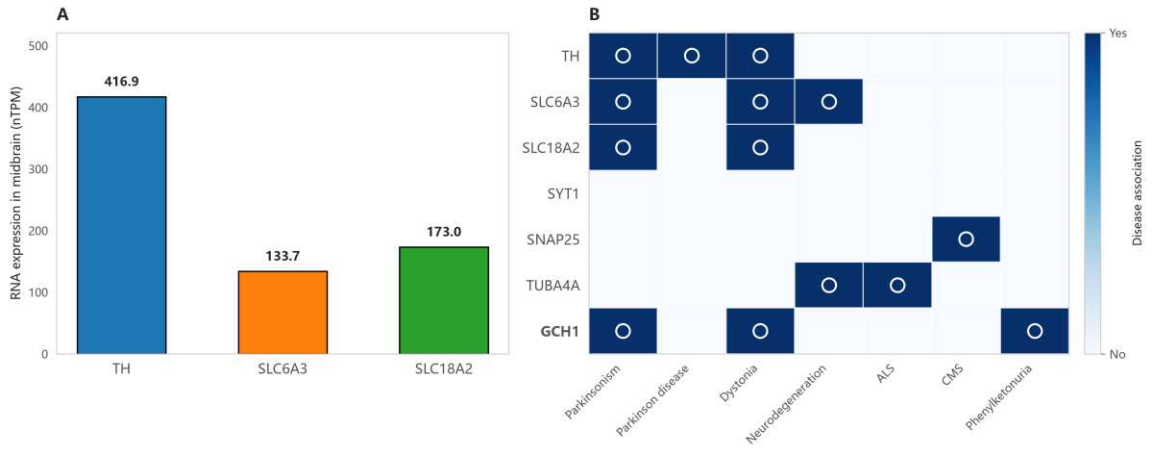

Figure 1. Dopaminergic-axis genes are highly expressed in the human midbrain and annotated across parkinsonian and related movement disorders. (A) Human Protein Atlas (HPA) RNA expression (nTPM) of TH, SLC6A3 and SLC18A2 in the midbrain, which

contains the substantia nigra. (B) HPA disease-association matrix for seven genes (TH, SLC6A3, SLC18A2, SYT1, SNAP25, TUBA4A, *GCH1*) across parkinsonism, Parkinson's disease, dystonia, neurodegeneration, amyotrophic lateral sclerosis, congenital myasthenic syndrome and phenylketonuria; white-ringed cells mark documented gene–disease associations, with *GCH1* annotated to parkinsonism, dystonia and phenylketonuria.

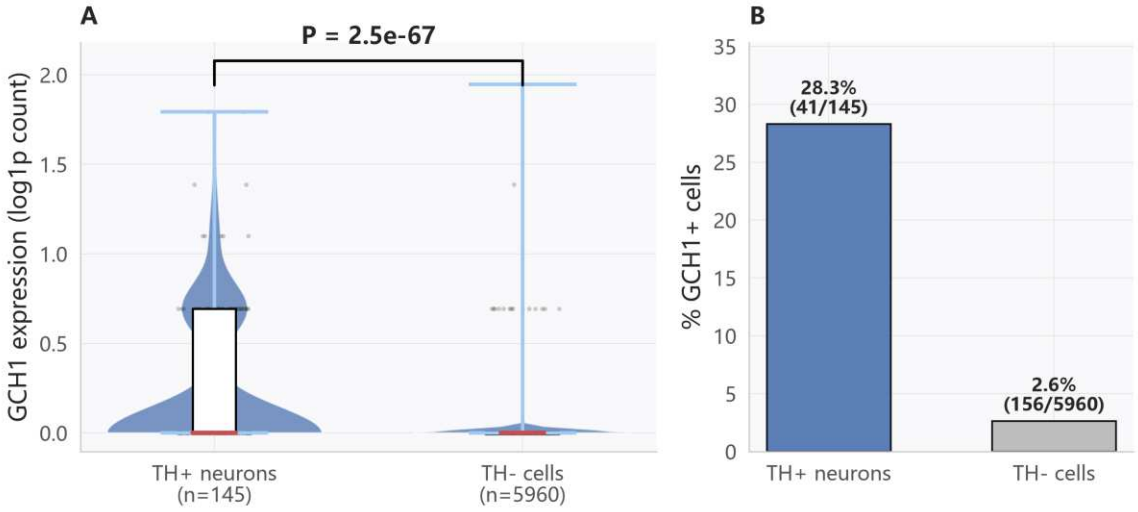

Figure 2. *GCH1* is co-expressed with TH in human substantia nigra dopaminergic neurons. Single-nucleus RNA-seq analysis of a published human substantia nigra atlas (GSE140231; n = 6,105 nuclei from five control donors). (A) *GCH1* expression (log1p-transformed counts) in TH-positive neurons (n = 145) versus TH-negative cells (n = 5,960); Mann–Whitney U test, $P < 0.0001$. (B) Percentage of *GCH1*-positive cells among TH-positive neurons (28.3%) versus TH-negative cells (2.6%).

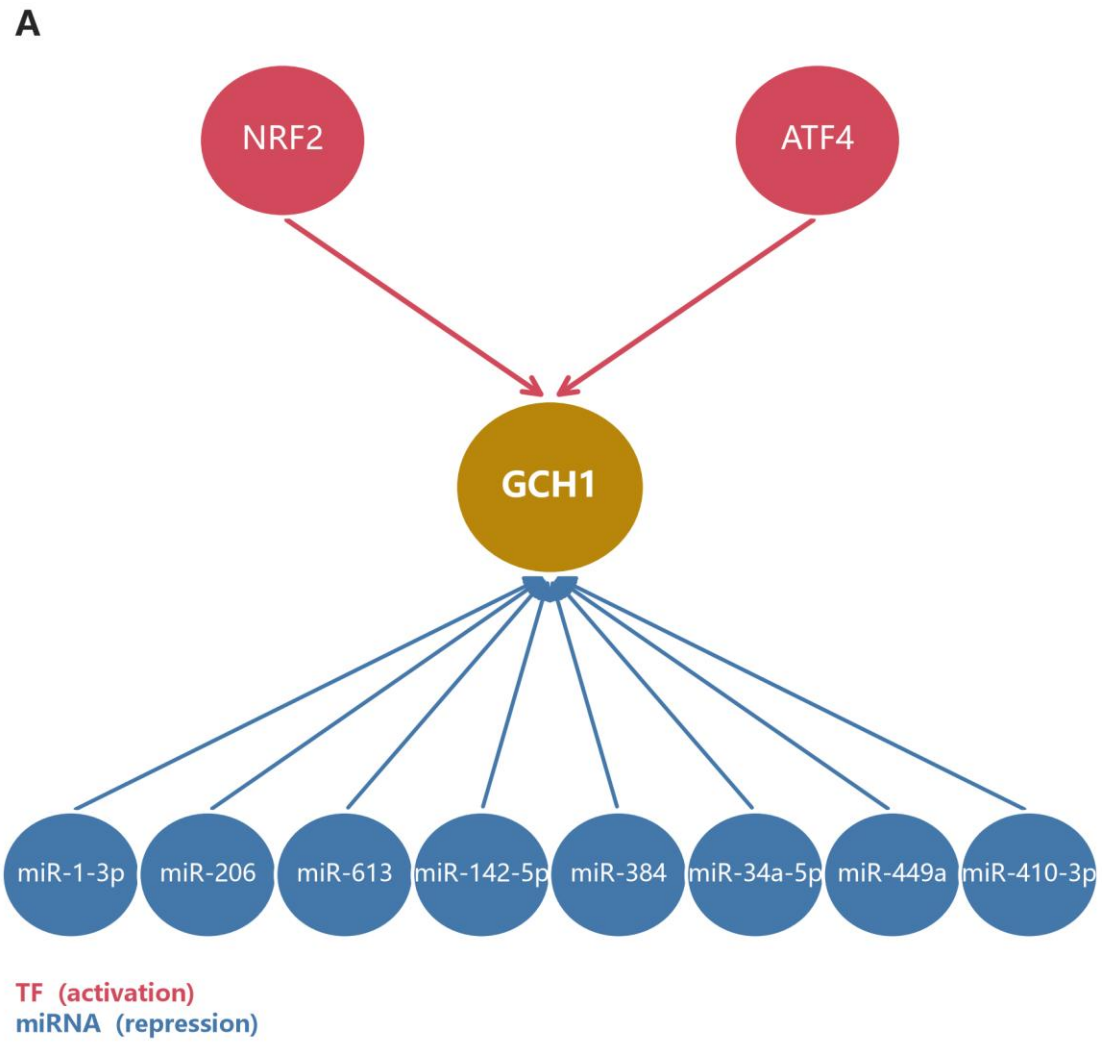

Figure 3. *GCH1* regulatory network. Transcription factors NRF2 (NFE2L2) and ATF4 activate *GCH1*: NRF2 directly binds the *GCH1* promoter (chromatin immunoprecipitation-validated), and ATF4 regulates *GCH1* through the integrated stress response. Multiple microRNAs are predicted to target *GCH1* (ENCORI/starBase, CLIP experimental evidence) and are shown as candidate post-transcriptional regulators pending functional validation. Red arrows, transcriptional activation; dashed blue arrow, predicted post-transcriptional repression.

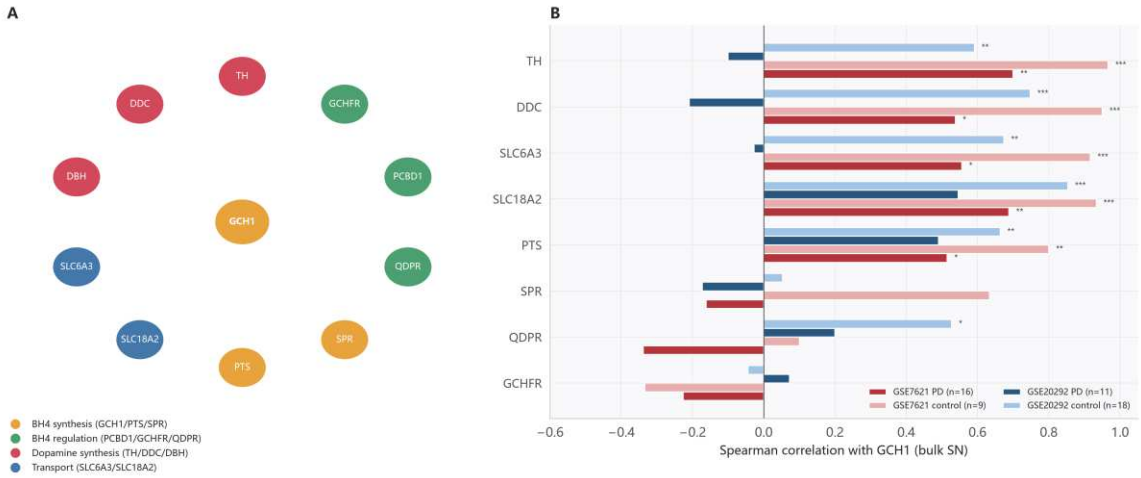

Figure 4. *GCH1*-centered protein–protein interaction (PPI) network and expression co-expression validation. (A) PPI network assembled from STRING (combined score ≥ 0.4); edge thickness reflects interaction confidence; nodes are colored by functional module. (B) Spearman correlation between *GCH1* and its interaction partners in two independent bulk substantia nigra cohorts, shown for all samples and stratified by PD versus control status (GSE7621: 16 PD, 9 controls; GSE20292: 11 PD, 18 controls). Note the attenuation of the *GCH1*–TH/DDC/SLC6A3 co-expression coupling in the PD subgroup. *P < 0.05, **P < 0.01, ***P < 0.001.

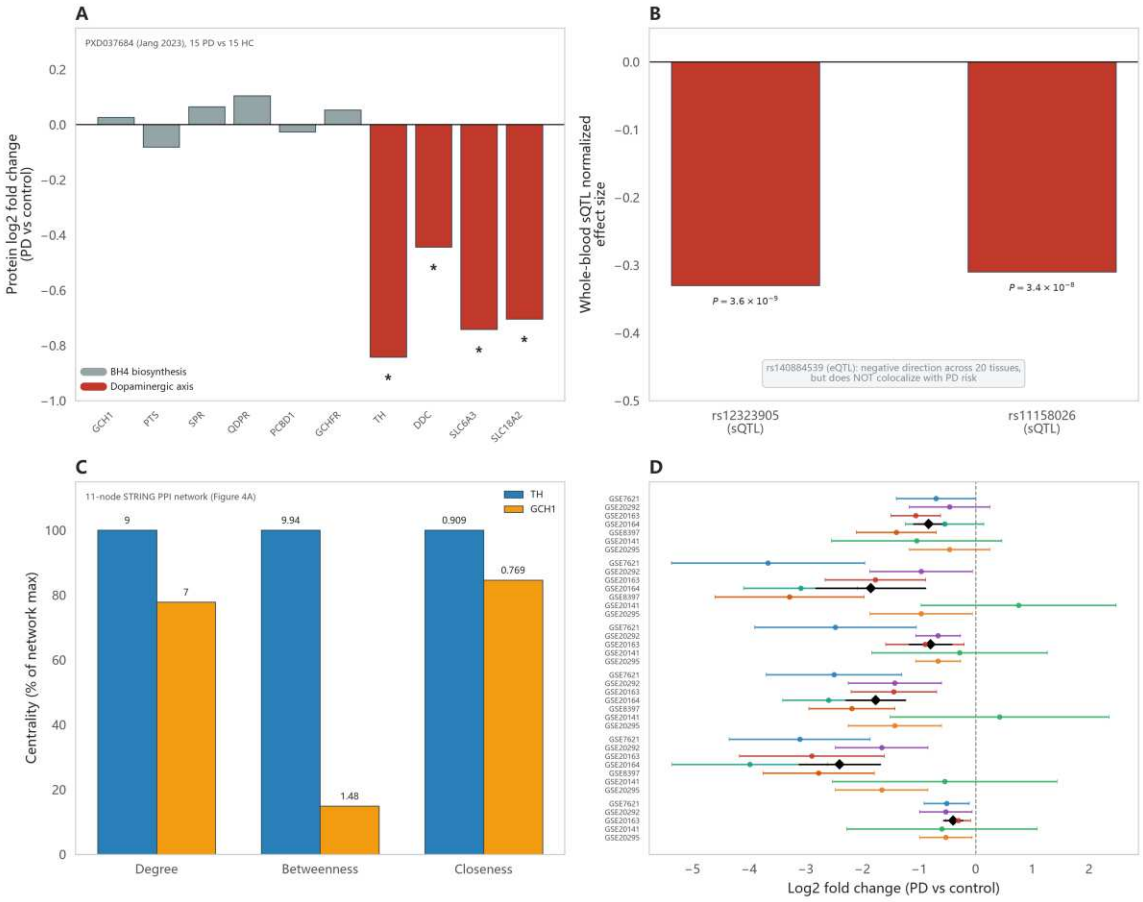

Figure 5. *GCH1* acts in PD through function rather than abundance. (A) Protein abundance (log2 fold change, PD vs control) of the six BH4 biosynthetic enzymes (*GCH1*, PTS, SPR, QDPR, PCBD1, GCHFR) and the four dopaminergic-axis proteins (TH, DDC, SLC6A3, SLC18A2) in a quantitative proteomic dataset (PXD037684, Jang et al. 2023; 15 PD, 15 controls); BH4 enzymes are unchanged ($q > 0.24$), whereas the dopaminergic proteins are significantly reduced (*$q < 0.05$). (B) GTEx v8 whole-blood splicing QTL normalized effect sizes for the two PD-associated *GCH1* variants rs12323905 and rs11158026; the expression QTL rs140884539 shows a consistently negative direction across 20 tissues but does not colocalize with PD risk. (C) Topological centrality (degree, betweenness, closeness) of TH versus *GCH1* in the 11-node STRING PPI network, relative to the network maximum; TH is the topological center, whereas *GCH1* ranks fourth. (D) Random-effects (DerSimonian–Laird) meta-analysis of *GCH1* and dopaminergic-axis genes across seven substantia nigra cohorts (GSE7621,

GSE20292, GSE20163, GSE20164, GSE8397, GSE20141, GSE20295); filled circles, per-cohort log2 fold change with 95% CI; black diamonds, pooled effect.

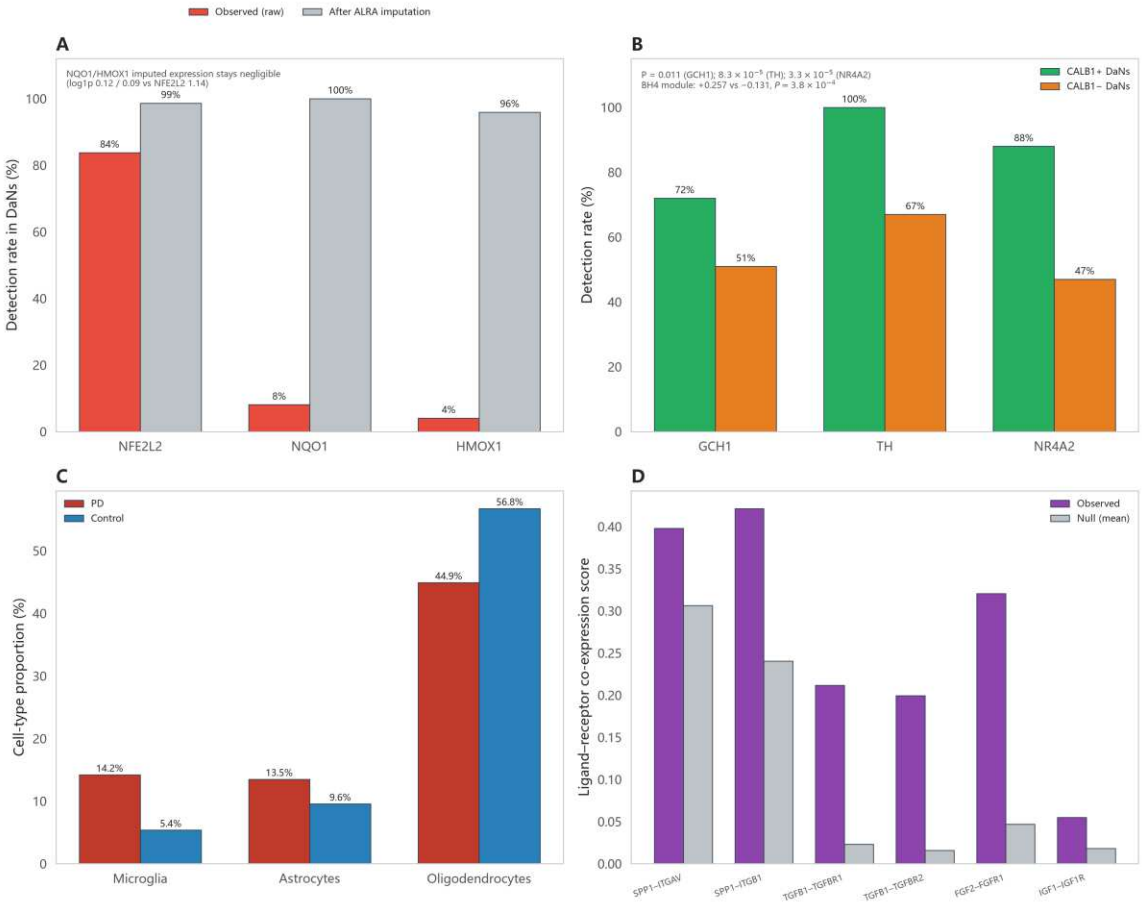

Figure 6. A non-cell-autonomous layer in the PD midbrain (GSE157783). (A) Detection rate of NFE2L2, NQO1 and HMOX1 in dopaminergic neurons (DaNs) before and after ALRA imputation; the NRF2 transcription factor is detected in 84% of DaNs, whereas its antioxidant effectors NQO1 (8%) and HMOX1 (4%) are barely detected, and their imputed expression remains negligible (log1p 0.12 and 0.09 versus NFE2L2 1.14). Detection-rate benchmarks against positive-control DaN markers (mean 60.0%; e.g., TH 78.4%, SLC18A2 83.8%) and negative-control genes (mean 16.6%; e.g., ALB 2.7%, CD3D 0%, MOG 4.1%) place NQO1 and HMOX1 near the negative-control floor, confirming that their low detection is biological rather than purely technical. (B) Detection rate of *GCH1*, TH and NR4A2 in CALB1+ versus CALB1− DaNs; the resistant CALB1+ subtype is enriched for the *GCH1*–BH4 axis. (C) Cell-type proportions

in PD versus control midbrain, showing glial expansion (microglia 14.2% vs 5.4%, astrocytes 13.5% vs 9.6%) and a proportional reduction of oligodendrocytes (44.9% vs 56.8%). (D) Ligand–receptor co-expression scores (ligand detection in microglia/astrocytes × receptor detection in DaNs) for six candidate glia→DaN pairs, observed versus null (1,000 permutations; empirical $P \leq 0.006$).

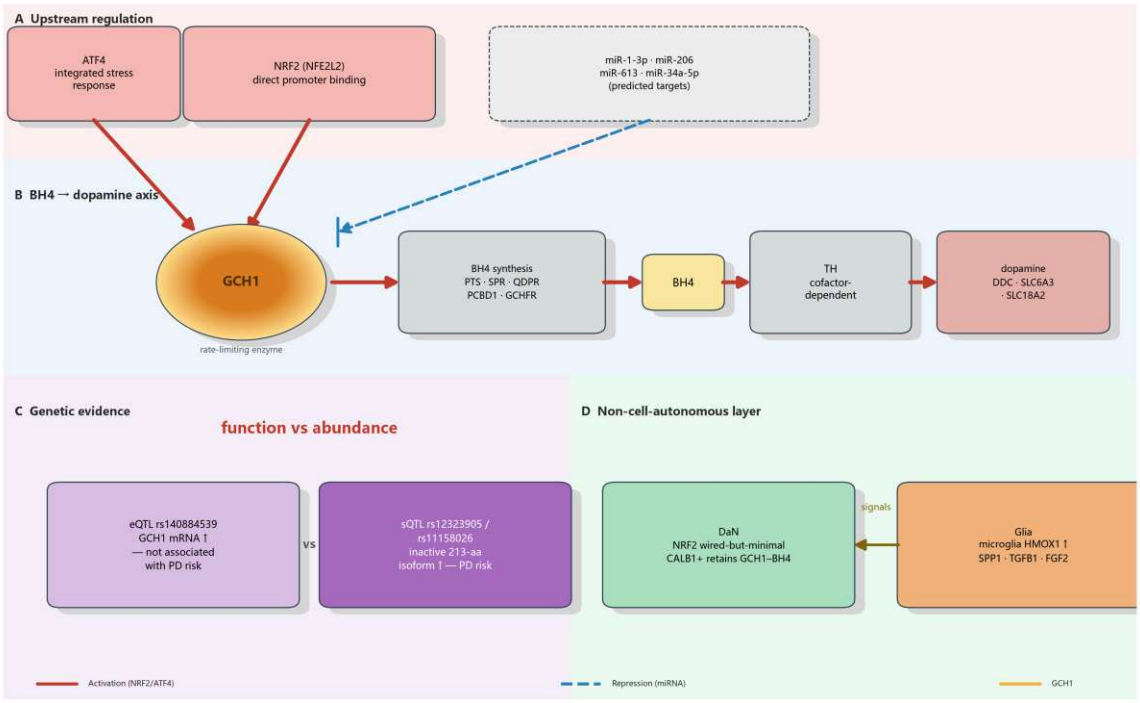

Figure 7. Mechanistic model of the *GCH1*–BH4 axis in Parkinson's disease. (A) Upstream regulation: NRF2 (NFE2L2) directly binds and activates the *GCH1* promoter, ATF4 activates *GCH1* through the integrated stress response, and multiple microRNAs (miR-1-3p, miR-206, miR-613, miR-34a-5p) are predicted to repress *GCH1*. (B) *GCH1* is the rate-limiting enzyme of BH4 synthesis (PTS, SPR, QDPR, PCBD1, GCHFR), and BH4 is the obligatory cofactor of TH for dopamine synthesis (DDC, SLC6A3, SLC18A2). (C) Genetic evidence distinguishes function from abundance: the expression QTL rs140884539 raises *GCH1* mRNA but is not associated with PD, whereas the splicing QTL rs12323905/rs11158026 generates a catalytically inactive 213-amino-acid isoform and colocalizes with PD risk. (D) A non-cell-autonomous layer: dopaminergic neurons show a wired-but-minimal NRF2 antioxidant program and the resistant CALB1+

subtype retains the *GCH1*–BH4 axis, whereas microglia express HMOX1 and candidate glia-to-DaN signals (SPP1, TGFB1, FGF2) are identified. Red, activation; blue dashed, predicted repression.

Supplementary Files

This is a list of supplementary files associated with this preprint. Click to download.

- SupplementaryMaterial.docx